Systems/Circuits

Pumilio-2 Regulates Translation of $Na_v1.6$ to Mediate Homeostasis of Membrane Excitability

Heather E. Driscoll, Nara I. Muraro, Miaomiao He, and Richard A. Baines
Faculty of Life Sciences, University of Manchester, Manchester M13 9PT, United Kingdom

The ability to regulate intrinsic membrane excitability, to maintain consistency of action potential firing, is critical for stable neural circuit activity. Without such mechanisms, Hebbian-based synaptic plasticity could push circuits toward activity saturation or, alternatively, quiescence. Although now well documented, the underlying molecular components of these homeostatic mechanisms remain poorly understood. Recent work in the fruit fly, *Drosophila melanogaster*, has identified Pumilio (Pum), a translational repressor, as an essential component of one such mechanism. In response to changing synaptic excitation, Pum regulates the translation of the voltage-gated sodium conductance, leading to a concomitant adjustment in action potential firing. Although similar homeostatic mechanisms are operational in mammalian neurons, it is unknown whether Pum is similarly involved. In this study, we report that Pum2 is indeed central to the homeostatic mechanism regulating membrane excitability in rat visual cortical pyramidal neurons. Using RNA interference, we observed that loss of Pum2 leads to increased sodium current (I_{Na}) and action potential firing, mimicking the response by these neurons to being deprived of synaptic depolarization. In contrast, increased synaptic depolarization results in increased Pum2 expression and subsequent reduction in I_{Na} and membrane excitability. We further show that Pum2 is able to directly bind the predominant voltage-gated sodium channel transcript ($Na_V1.6$) expressed in these neurons and, through doing so, regulates translation of this key determinant of membrane excitability. Together, our results show that Pum2 forms part of a homeostatic mechanism that matches membrane excitability to synaptic depolarization in mammalian neurons.

Introduction

Neuronal homeostasis enables neurons to adapt to changing synaptic excitation, to maintain consistency despite rapid turnover of ion channels and to compensate for perturbations in network activity. Without homeostasis, Hebbian-based changes in synaptic efficacy have the potential to destabilize circuit activity. Compensatory mechanisms operate to prevent this by maintaining membrane excitability within physiologically relevant limits (Turrigiano et al., 1994; Turrigiano, 1999). Homeostatic mechanisms fall into two broad categories: synaptic and intrinsic. Synaptic mechanisms encompass the alteration of neurotransmitter release (Turrigiano and Nelson, 2004; Erickson and Spana, 2006) and/or postsynaptic receptor expression (Ehlers, 2003). In contrast, neurons can alter their membrane excitability through intrinsic changes in expressed voltage-gated ion channels (Turrigiano and Nelson, 1998; Desai et al., 1999; Baines, 2003; Zhang and Linden, 2003; Marder and Goaillard, 2006).

Received March 1, 2013; revised April 18, 2013; accepted April 26, 2013.

Author contributions: H.E.D., N.I.M., and R.A.B. designed research; H.E.D., N.I.M., and M.H. performed research; H.E.D. and R.A.B. analyzed data; H.E.D., N.I.M., and R.A.B. wrote the paper.

This work was supported by Wellcome Trust Grant 088720. We are indebted to Drs. Paolo Macchi, Michael Kiebler, and G. Turrigiano for advice and reagents. We thank Drs. Verena Wolfram and Anne-Kathrin Streit for commenting on this manuscript and advice throughout the project. We also thank Drs. Wei-Hsiang Lin and Richard Marley and other members of the Baines group for their help and advice during the course of this work.

Correspondence should be addressed to Richard Baines, Faculty of Life Sciences, University of Manchester, Oxford Road, Manchester M13 9PT, UK. E-mail: Richard.Baines@manchester.ac.uk.

N. I. Muraro's present address: Laboratory of Behavioral Genetics, Institute Leloir Foundation/Institute of Biochemical Investigations-Buenos Aires, Avenida Patricias Argentinas 435, 1405-BWE Buenos Aires, Argentina.

DOI:10.1523/JNEUROSCI.0921-13.2013

 0270-6474/13/339644-11$15.00/0

Most forms of intrinsic mechanisms involve changes in the relative density or functional properties of ion channels. A common target is the voltage-gated sodium channel (Na_v) (Desai et al., 1999; Mee et al., 2004; Muraro et al., 2008). Sodium channels are critical for the generation of action potentials, and alterations in their density can change action potential threshold (Catterall et al., 2005; Kole et al., 2008). Our work in *Drosophila* shows that changes in synaptic depolarization of motoneurons are compensated for by altered membrane excitability, primarily mediated through a change in sodium current (I_{Na}) density (Baines et al., 2001; Baines, 2003; Mee et al., 2004; Muraro et al., 2008). This change requires Pumilio (Pum), a known translational repressor (Tautz, 1988; Wharton and Struhl, 1991; Wharton et al., 1998). The *Drosophila* model is consistent with activity-dependent change in Pum acting to regulate translation of the sole Na_v (termed *paralytic*) in this insect. As synaptic depolarization increases, so does the activity of Pum, which, through binding to conserved domains [Nanos response elements (NREs)] in the Na_v transcript, suppress translation (Muraro et al., 2008). This reduces I_{Na} and action potential firing.

Mammalian cortical neurons similarly exhibit intrinsic homeostatic regulation of I_{Na} (Desai et al., 1999), and Pum2 expression is activity dependent in cultured hippocampal neurons (Vessey et al., 2006). Alignment of mouse Pum1 and Pum2 proteins with their *Drosophila* homolog show 51 and 55% overall similarity, which further increases to 86 and 88% in the RNA-binding domains (Spassov and Jurecic, 2002). Pum2 has been reported to bind rat $Na_v1.1$ transcript (Vessey et al., 2010). However, whether Pum2 regulates membrane excitability in mamma-

lian neurons in an activity-dependent manner, akin to that observed in *Drosophila*, is unknown.

We show here that cultured rat cortical pyramidal neurons regulate both I_{Na} and action potential firing in response to changing synaptic depolarization. Activity also affects the expression of Pum2, and, moreover, manipulation of Pum2 is sufficient to alter I_{Na} and action potential firing. We further show that Pum2 directly binds *$Na_V1.6$* mRNA, which is the principal *Na_v* expressed in these neurons. We conclude that Pum2 is an essential component of the homeostatic mechanism that allows neurons to regulate intrinsic excitability to adapt to changes in synaptic depolarization.

Materials and Methods

Cell culture and transfection. Visual cortical neurons were isolated from 3-d-old (P3) Sprague Dawley rat pups of either sex. Pups were killed by decapitation. All experiments were conducted in accordance with the United Kingdom Animals Scientific Procedures Act (1986) and institutional regulations. The visual cortex was removed and placed in ice-cold ACSF buffer (in mM: 126 NaCl, 3 KCl, 2 $MgSO_4.7H_2O$, 1 $NaH_2PO_4.2H_2O$, 25 $NaHCO_3$, 2 $CaCl_2$, and 14 dextrose, pH 7.4), sliced into 500-μm-thick sections, and incubated in 20 U/ml papain (Worthington Biochemical) in Earle's balanced salt solution (1.8 mM calcium EBSS supplemented with 10 mM dextrose) for 90 min at 37°C in a 5% CO_2 humidified incubator. After digestion, tissue was resuspended in weak protease inhibitor (1 mg/ml of both BSA and trypsin inhibitor in EBSS) and an equal amount of strong inhibitor solution (10 mg/ml of both BSA and trypsin inhibitor in EBSS) was added. The tissue was triturated with a fire-polished Pasteur glass pipette. After any remaining tissue had settled, the supernatant was removed and filtered through a 70 μm mesh (Falcon; BD Biosciences Discovery Labware) and centrifuged at 1000 $\times$ *g* for 5 min at room temperature. Dissociated cells were resuspended in MEM cell culture medium (supplemented with 5% FBS, 2 mM L-glutamine, 50,000 U/50 mg penicillin–streptomycin, 1$\times$ B27 supplement, and 33 mM dextrose) and plated onto poly-D-lysine (0.5 mg/ml; Sigma) and collagen-1 (0.782 mg/ml; rat tail collagen; BD Biosciences) coated 22 $\times$ 22 mm glass coverslips at a density of 1.5×10^5 cells/ml. One-third of the media was refreshed every 2 d.

To assess the role of Pum2, cortical neurons were transfected with an RNA interference (shRNA) plasmid (also encoding a GFP reporter) against Pum2 or empty pSUPERIOR–GFP as control using the calcium phosphate precipitation technique after 7–9 d in culture as described by Vessey et al. (2010). Plasmid DNA (3 μg) was added to freshly diluted $CaCl_2$ solution (250 mM), and the total volume of both solutions was 60 μl. An equal amount of 2$\times$ 2-[bis(2-hydroxyethyl)amino]ethanesulfonic acid (BES) buffer (in mM: 50 BES, 1.5 Na_2HPO_4, and 280 $NaCl_2$, pH 7.2) was added in a dropwise manner to the DNA/$CaCl_2$ solution. The DNA/calcium phosphate solution was immediately added dropwise to the neurons growing in 3 cm Petri dishes containing 2 ml of prewarmed transfection medium (MEM supplemented with 1 mM sodium pyruvate, 15 mM HEPES, 2 mM L-glutamate, 1$\times$ B27 supplement, and 33 mM dextrose), followed by gentle swirling. Neurons were incubated at 37°C in 5% CO_2 for 40 min to allow the DNA/calcium phosphate coprecipitate to form. Neurons were washed with prewarmed HBSS buffer (in mM: 135 $NaCl_2$, 20 HEPES, 4 KCl, 1 Na_2HPO_4, 2 $CaCl_2$, 1 $MgCl_2$, and 10 glucose, pH 7.3) for 5 min to remove the DNA/calcium phosphate coprecipitate. Transfected cortical neurons were maintained in culture medium for an additional 2–3 d.

Electrophysiology. Cortical neurons were visualized at 40$\times$ with differential interference contrast optics, and transfection was confirmed by GFP expression. Patch-clamp recordings were obtained using thick-walled borosilicate glass electrodes (GC100F-10; Harvard Apparatus) with resistance between 3 and 5 MΩ. Pyramidal neurons were identified by shape and large soma size. Recordings were made using a Multiclamp 700A amplifier controlled by pClamp 10.2 (Molecular Devices). To better resolve I_{Na}, an online leak subtraction protocol was used (P/4). Traces were filtered at 10 kHz (Bessel) and digitized at 20 kHz.

Whole-cell voltage clamp was used to isolate I_{Na}. Cells were exposed to an extracellular solution containing the following (in mM): 33 NaCl, 97 choline chloride, 3 KCl, 2 $MgCl_2$, 20 HEPES, 1.6 $CaCl_2$, 0.4 $CdCl_2$, 10 tetraethylammonium chloride, 5 4-aminopyridine, and 14 dextrose, pH 7.4. Internal patch solution contained the following (in mM): 120 $CsMeSO_4$, 10 KCl, 10 HEPES, 10 EGTA, and 3 ATP disodium salt, pH 7.3. To activate voltage-gated sodium channels, neurons were stepped from a holding potential of -60 to $+30$ mV in 5 mV increments for 50 ms from a prepulse of -90 mV (100 ms). Each neuron was subjected to three separate activation protocols, and an average was generated. Current density was obtained by normalizing to cell capacitance (69.14 $\pm$ 5.79 vs 63.62 $\pm$ 5.61 vs 70.03 $\pm$ 8.69 pF, control vs activity-deprived, $n = 26$ and 21, $p = 0.61$, control vs activity-enhanced, $n = 26$ and 19, $p = 0.10$). Current–voltage plots shown are averages derived from three separate cultures with a minimum of eight recordings from each individual culture.

Whole-cell current-clamp recordings were performed using external saline containing the following (in mM): 126 NaCl, 3 KCl, 2 $MgSO_4.7H_2O$, 1 $NaH_2PO_4.2H_2O$, 25 $NaHCO_3$, 2 $CaCl_2$, and 14 dextrose, pH 7.4 (maintained by bubbling continuously with 5% CO_2/ 95% O_2). Internal patch solution used contained the following (in mM): 130 $KMeSO_4$, 10 KCl, 10 HEPES, 2 $MgSO_4.7H_2O$, 0.5 EGTA, and 3 ATP disodium salt, pH 7.3. After breakthrough, neurons were held at -60 mV by injection of constant current. Current injections of -20 to $+200$ pA in 20 pA increments were applied for 500 ms. For each neuron, this protocol was repeated twice, and the number of action potentials fired at each step was averaged. Input–output curves shown are averages derived from at least two separate cultures with a minimum of eight recordings from each individual culture.

Manipulation of synaptic activity and Pum2 silencing. For chronic block of excitatory (mediated by glutamate) or inhibitory (mediated by GABA) synaptic currents, NBQX/AP-5 (20 and 50 μM, respectively) or gabazine (40 μM SR95531) were added to cell cultures on day 7 (drugs from Abcam). After 24 h, a third of the media was exchanged and drugs were refreshed. Cultures were maintained for an additional 24 h. Drugs were washed out before recordings. For experiments to assess the role of Pum2, cortical neurons were transfected with plasmids to express either shRNA against Pum2 (also containing GFP) or empty pSUPERIOR–GFP as a control, as described above. When transfection and antagonists were used in combination, neurons were transfected and incubated overnight and then treated with drugs for 2 d, as detailed above.

RT-PCR from whole tissue. P3 rat visual cortex was homogenized, RNA was extracted using an RNeasy Plus Micro Kit (Qiagen) following the instructions of the manufacturer, and cDNA was synthesized using the Revert Aid H Minus first-strand cDNA synthesis kit (Fermentas Life Sciences). The procedure used was as follows. Briefly, 1 μl of 25 ng/μl cDNA samples were amplified for 35 cycles in the presence of individual sets of primer pairs (Table 1). To detect product, 5 μl of amplified cDNA was separated by 2% agarose gel electrophoresis, visualized by ethidium bromide (1 μg/ml) under ultraviolet light. The PCR product was excised from the agarose gel after electrophoresis and purified using the QIAquick Gel Extraction Kit (Qiagen). The PCR product was sequenced using Big Dye Terminator Version 3.1 Chemistry and the primers described in Table 1, and run on an ABI PRISM 3130xl Genetic Analyzer (Applied Biosystems).

RT-PCR from pyramidal neurons. In whole-cell configuration, gentle suction was applied to aspirate the cytoplasm without disrupting the seal. The tip of the electrode containing the aspirated cell content was broken off in a 0.2 ml PCR tube containing RNase inhibitor and RNA-free water in a 1:4 ratio (5 μl total volume). cDNA (from 10 cells per sample) was synthesized using the Revert Aid H Minus first-strand cDNA synthesis kit (Fermentas Life Sciences). The synthesized cDNA was amplified using BIOTAQ DNA polymerase (Bioline). Controls were performed by placing patch pipettes next to transfected cells and using gentle suction to draw off a small amount of extracellular media. A two-stage PCR amplification was used: briefly, one-sixth of the cDNA product was amplified for 45 cycles in the presence of six Na_v primers (Table 1). The thermal cycling protocol was 2 min at 94°C, 45 cycles at 15 s at 94°C, 30 s at 48°C, and finally 50 s at 72°C, followed by a 10 min final extension. In the second-stage PCR, 1 μl of the first-stage PCR amplification was used as

Table 1. Primer sequences used to PCR amplify Na_v transcripts

mRNA (RefSeq accession number)	Start position (nt)	Product size (bp)	Primer (5′ to 3′)
Na_V1.1 (NM_030875.1)			
Forward	4394	583	tggtgacacatttgagatcacc
Reverse			tacgtgacaaaatgcttgtcacataa
Na_V1.2 (NM_012647.1)			
Forward	4324	574	ggggaaatgtttgatgtgagc
Reverse			aggatgttggtcatctcctga
Na_V1.3 (NM_013119.1)			
Forward	4367	576	gacaacaggcaacatgtttgaaataaaa
Reverse			ggacaaaaccagggtcatgtatttt
Na_V1.5 (NM_013125.2)			
Forward	4313	570	cctgcctctgaactacacc
Reverse			caagatgttgaccttctcagg
Na_V1.6 (NM_019266.2)			
Forward	4245	583	tgaaatccggttcgaaatcgatatt
Reverse			agtaaagaatgttctccatctgctt
Na_V1.8 (NM_017247.1)			
Forward	4160	574	attttccaacgtgaattcgacgat
Reverse			ccagaaccttcgtcttctcc

template, and an individual set of primer pairs were run for 40 cycles (for primers used, see Table 1).

Immunocytochemistry. Neurons were washed in PBS (in mM: 137 NaCl, 2.7 KCl, 8 Na_2HPO_4, and 1.46 KH_2PO_4, pH 7.4) and fixed in 4% paraformaldehyde for 15 min at room temperature. Neurons were permeabilized for 30 min in PBS containing 100 mM glycine, 1% BSA, and 0.2% Triton X-100 and then blocked for 1 h in PBS containing 300 mM glycine, 3% BSA, and 0.2% Triton X-100 at room temperature. The primary antibodies used were anti-Na_V1.6 (1:50; Alamone Labs), anti-Pum2 antibody (1:200; Abcam), and anti-microtubule-associated protein 2 antibody (1:1000; Sigma) diluted in PBS containing 10% normal goat serum and 0.2% Triton X-100 and incubated overnight at 4°C. Neurons were washed and incubated in Alexa Fluor 568 goat anti-rabbit IgG antibody (1:500; Molecular Devices, Invitrogen) and Alexa Fluor 488 goat anti-mouse IgG antibody (1:2000; Molecular Devices, Invitrogen) for 1 h at room temperature. Neurons were washed and mounted in Vectashield HardSet Mounting Medium (Vector Laboratories), and images were captured using a Leica DM6000B microscope. Captured *Z*-stacks were deconvolved, and soma fluorescence was measured using a circular region of interest tool in Image Pro 7 (Media Cybernetics). Fluorescent intensity data presented are corrected for both soma area (by dividing pixel intensity by area) and background values (by subtraction).

Immunoprecipitation. P3 rat brain was homogenized in ice-cold lysis buffer [25 mM HEPES, 150 mM KCl, 20 mM $MgCl_2$, 8% (v/v) glycerol, 0.1% (v/v) Nonidet P-40, 1 mM DTT, RNase inhibitor (1 U/μl; Thermo Fisher Scientific), and protease inhibitor (1:100; Sigma), pH 7.4]. Lysate was maintained at 4°C for 2 h with constant agitation and centrifuged for 20 min at 12,000 × *g* at 4°C, and supernatant was collected. Lysate was precleared using goat serum (50 μl/ml; Sigma) incubated for 1 h at 4°C with constant agitation, and 100 μl of Protein A Sepharose (100 μl/ml; GE Healthcare, Buckinghamshire, UK) was added and gently mixed for 1 h at 4°C. Lysate was centrifuged for 20 s at 12,000 × *g*, and supernatant was collected. Affinity-purified anti-Pum2 antibody (5 μg/mg; Abcam) or anti-pan-sodium channel antibody (6 μg/mg; Alamone Labs) was added to precleared lysate and incubated for 1 h at 4°C with constant agitation. Protein A Sepharose (200 μl/ml) was added and gently mixed for 1 h at 4°C. Lysate was centrifuged for 20 s at 12,000 × *g*, and the pellet was saved. Pellet was washed three times with fresh ice-cold lysis buffer, after each wash, the lysate was centrifuged for 20 s at 12,000 × *g*, and supernatant was discarded.

To isolate total RNA, the pellet was treated with TRIzol (Invitrogen) following the instructions of the manufacturer, and cDNA was synthesized using the Revert Aid H Minus first-strand cDNA synthesis kit (Fermentas Life Sciences). The synthesized cDNA was amplified in a two-stage PCR amplification as described previously.

Statistics. Statistical significance was calculated using a one-way ANOVA (with Bonferroni's *post hoc* comparison test) unless noted otherwise. Significance levels of $^*p \leq 0.05$ or $^{**}p \leq 0.01$ are shown.

Results

Activity blockade increases intrinsic excitability

Cortical pyramidal neurons deprived of synaptic excitation respond by lowering their threshold for action potential firing (Desai et al., 1999). This change in intrinsic excitability allows neurons to maintain consistency in firing when exposed to chronic changes in synaptic depolarization. However, although well documented, the underlying mechanism of this homeostatic response has not been fully investigated.

To determine the effects of chronic changes in activity on intrinsic electrical properties, we treated our pyramidal cell cultures for 48 h with either blockers of excitatory synaptic activity ("activity-deprived," NBQX/AP-5 at 20 and 50 μM, respectively) or blockers of inhibitory synaptic signaling ("activity-enhanced," gabazine at 40 μM). After washout of blockers, we used current-clamp recordings to determine input–output curves for action potential firing. Resting membrane potential, on breakthrough, was −46.0 ± 2.2, −33.8 ± 2.8, and −33.2 ± 3.5 mV (control vs activity-deprived vs activity-enhanced, $p = 0.01$ for activity manipulations compared with control but $p > 0.05$ for activity-deprived vs enhanced, $n \geq 8$, means ± SEM). Hyperpolarizing constant current was injected to hold V_m at −60 mV, a level at which all recorded cells were silent. Current injections were applied to depolarize cells to evoke action potential firing. Chronic activity deprivation (NBQX/AP-5) resulted in increased action potential firing compared with controls (Fig. 1*A*). At current amplitudes above 20 pA, the average frequency of firing was significantly greater than the average control frequency ($p = 9.92 \times 10^{-4}$; Fig. 1*B*). In contrast, exposure to enhanced excitation (gabazine) resulted in decreased action potential firing (Fig. 1*A*). At each current amplitude above 80 pA, the average frequency of firing was significantly decreased compared with control ($p = 0.05$; Fig. 1*B*). Threshold for action potential firing compared with control did not differ significantly in either treatment (−35.3 ± 1.7 vs −30.5 ± 2.1 vs −41.7 ± 2.3 mV; control vs activity-deprived vs activity-enhanced, $p > 0.05$ vs control, $n \geq 8$, means ± SEM). However, threshold was significantly different between the two activity manipulations ($p = 0.002$ activity-deprived vs activity-enhanced). Input resistance did not change (690 ± 70, 730 ± 90, and 790 ± 130 MΩ, control vs activity-deprived, $n = 20$ and 16, $p = 0.95$; control vs activity-enhanced, $n = 20$ and 14, $p = 0.76$). Thus, we conclude that deprivation of synaptic excitation results in increased action potential firing and vice versa.

Under voltage clamp, we observed that the average amplitude of I_{Na} was significantly increased after chronic activity deprivation (Fig. 2*A*). On average, activity deprivation increased peak I_{Na} by ~30% (−44.7 ± 4.1 vs −34.5 ± 2.0 pA/pF, deprived vs control, $n = 42$ and 22, $p = 0.02$; Fig. 2*B*). As predicted, exposure to enhanced excitation (gabazine) reduced the amplitude of I_{Na} (−34.5 ± 2.0 vs −15.7 ± 2.2 pA/pF, control vs enhanced, $n = 42$ and 20, $p = 1.66 \times 10^{-5}$; Fig. 2*A*,*B*). These observations, which confirm a previous report (Desai et al., 1999), show that the homeostatic response to changing levels of synaptic input is mediated, at least in part, by reciprocal change in I_{Na}. However, it is important to note that, in addition to I_{Na}, Desai et al. show that K^+ conductances are also affected, and it is likely that these combined changes account for the alteration to membrane excitability.

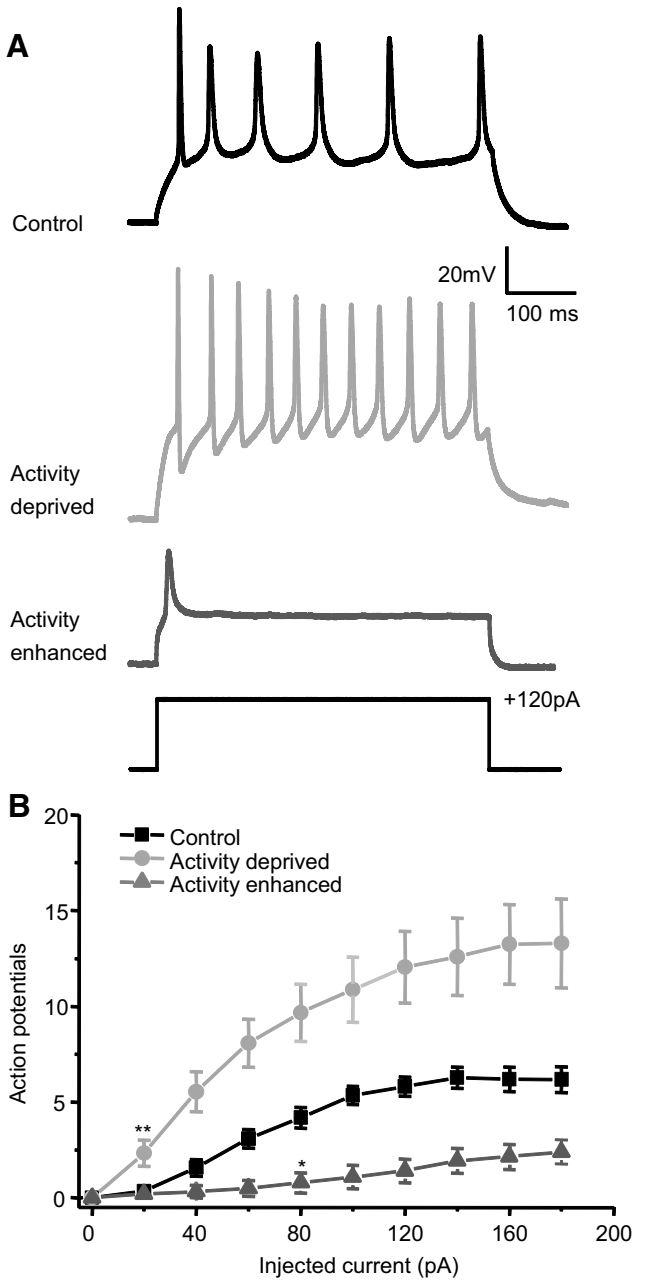

Figure 1. Chronic alteration of synaptic excitation changes intrinsic neuronal excitability. ***A***, Representative action potential firing evoked in whole-cell configuration by a 120 pA/500 ms current injection in pyramidal neurons grown under control (top black trace), activity-deprived (20 μM NBQX and 50 μM AP-5 treatment for 48 h; middle light gray trace) or activity-enhanced (40 μM gabazine treatment for 48 h; bottom dark gray trace) conditions. ***B***, Input–output plots depicting average number of action potentials fired versus amplitude of current injection (means ± SEM, $n \geq 8$). *$p \leq 0.05$ and **$p \leq 0.01$, the first level at which changes in action potential number are significantly different from control (one-way ANOVA with Bonferroni's *post hoc* comparison test).

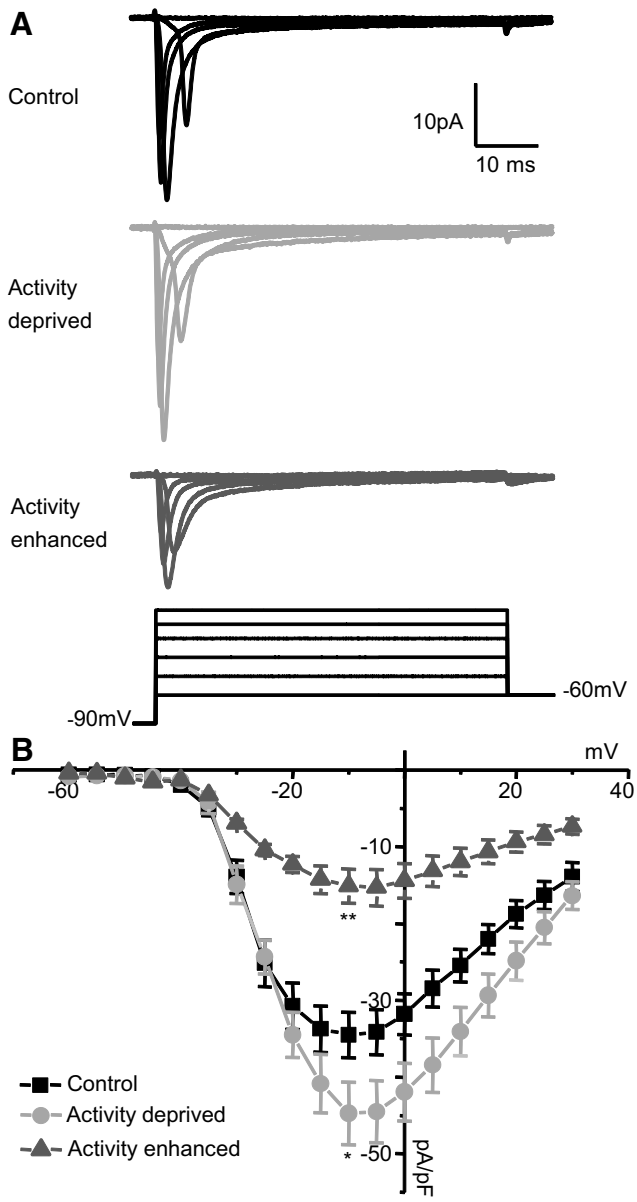

Figure 2. Chronic alteration of synaptic excitation changes I_{Na} amplitude. ***A***, Representative voltage-clamp recordings of I_{Na} in pyramidal neurons of control (top black trace), activity-deprived (middle light gray trace), and activity-enhanced (bottom dark gray trace) neurons. Voltage steps shown are to $V_m = -45, -25, -10, 5$, and 25 mV, respectively. ***B***, Current–voltage plots for I_{Na} measured after chronic activity blockade or enhanced activity (means ± SEM, $n \geq 19$). *$p \leq 0.05$ and **$p \leq 0.01$, peak I_{Na} is significantly different from control (one-way ANOVA with Bonferroni's *post hoc* comparison test).

Pum2 regulates intrinsic excitability in response to altered synaptic excitation

To establish whether Pum2 expression is altered after chronic block of either synaptic excitation (NBQX/AP-5) or inhibition (gabazine), we quantified Pum2 protein expression levels in pyramidal neurons under these conditions. To do this, we used immunofluorescence with an antibody to Pum2 (see Materials and Methods). Pum2 fluorescence intensity was significantly decreased in chronically activity-deprived neurons compared with control neurons (~44%: 8065.5 ± 274.6 vs 14,499.6 ± 1145.4 pixel intensity units, deprived vs control, $n = 25$ and 59, $p = 6.14 \times 10^{-12}$; Fig. 3*A*,*B*). In comparison, in cultures in which synaptic excitation was increased (gabazine), the average Pum2 fluorescence intensity was significantly increased (~58%: 16,606.7 ± 702.2 vs 10,462.9 ± 866.9 pixel intensity units, depolarized vs control, $n = 60$ and 55, $p = 1.09 \times 10^{-25}$; Fig. 3*A*,*B*). Control values are normalized to 1.0 in Figure 3*B*.

These data show that activity deprivation, which results in increased I_{Na} and action potential firing, is associated with a decrease in levels of Pum2 and vice versa. This is consistent with a model derived from *Drosophila* in which a reduction in Pum is associated with increased I_{Na} (Mee et al., 2004; Muraro et al.,

2008). To directly demonstrate that reduced Pum2 is sufficient to increase both I_{Na} and action potential firing, we used RNA interference (shRNA). Pum2 immunofluorescence intensity was significantly decreased in cells transfected with shRNA–Pum2, indicative of effective knockdown (control, 17,053.0 ± 1132.8 vs shRNA–Pum2, 7699.5 ± 406.8, $n = 21$ and 20, $p = 3.04 \times 10^{-10}$, *t* test). As expected, after transfection of pyramidal neurons with shRNA against Pum2, we observed a significant increase in action potential firing. At each current step above 20 pA, the average frequency of firing was significantly increased compared with control neurons transfected with an empty pSUPERIOR–GFP vector ($p = 0.003$, *t* test; Fig. 4*A*,*B*). We also observed a significant increase in I_{Na} in shRNA-treated cells (−68.2 ± 5.3 vs −31.6 ± 1.9 pA/pF, shRNA vs control, $n = 40$ and 70, $p = 5.89 \times 10^{-12}$, *t* test; Fig. 4*C*,*D*). These observations are consistent with Pum2 being sufficient to regulate both action potential firing and I_{Na} in response to changing synaptic excitation in pyramidal cells. We also attempted to overexpress Pum2 in our cultures, but cell viability was affected to the extent that it was not possible to obtain adequate patch recordings for analysis.

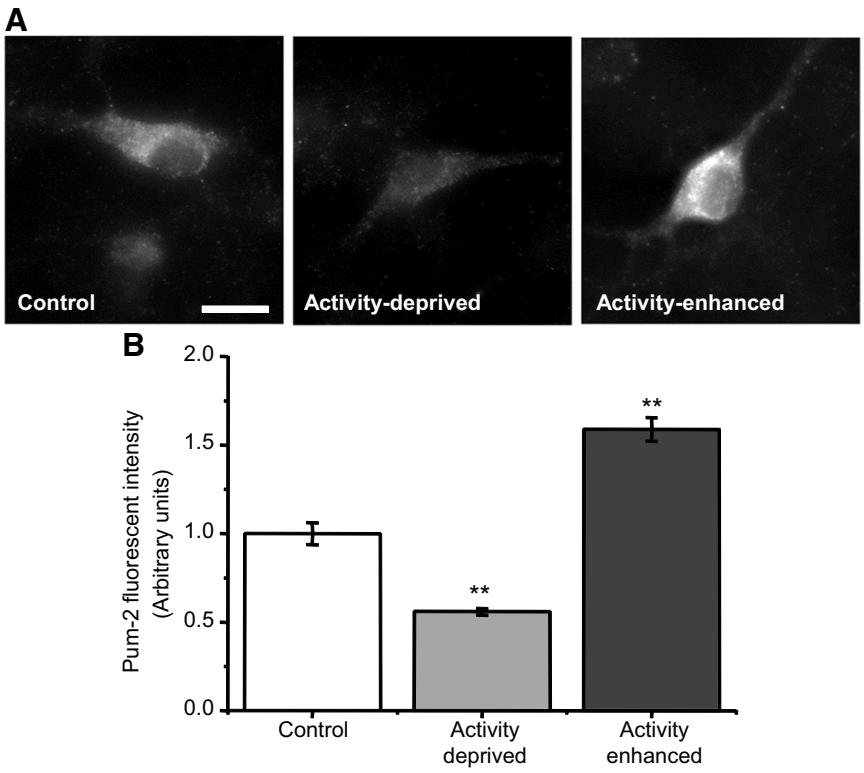

Figure 3. Synaptic excitation influences expression of Pum2. ***A***, Immunofluorescence for Pum2 in cortical pyramidal neurons shows reduced signal intensity in activity-deprived (middle image) and increased signal in activity-enhanced (right image) neurons compared with control conditions (left image). Scale bar, 50 μm. ***B***, Shows averaged data. Immunofluorescence for Pum2 is decreased by 44% in activity-deprived neurons and increased by 58% in activity-enhanced neurons. Immunofluorescence intensity measurements (measured at the cell body) were performed at the same time and normalized for cell surface area (for details, see Materials and Methods). Data shown are means ± SEM, $n \geq 25$, $^{**}p \leq 0.01$ (one-way ANOVA with Bonferroni's *post hoc* comparison test).

Our results show that reducing Pum2 recapitulates the effect of activity deprivation, with both treatments increasing I_{Na} and action potential firing. This suggests that Pum2 participates in the homeostatic mechanism triggered by activity deprivation. To confirm this, we adopted two approaches. First, we determined whether the change in membrane excitability mediated by activity deprivation (i.e., exposure to NBQX and AP-5) and Pum2 knockdown are synergistic. The two treatments would not be expected to show synergy if activity mediates its effect through a pathway involving Pum2. Our second approach combined Pum2–shRNA knockdown with chronic enhancement of synaptic activity (i.e., exposure to gabazine). We reasoned that, if enhanced activity results in reduced I_{Na} through increased Pum2, then this combination should prevent change to I_{Na}. We focused our attention on I_{Na} for this analysis, but it is inferred that any increase in I_{Na} leads to a concomitant increase in action potential firing (Mee et al., 2004; Muraro et al., 2008).

Two-way ANOVA revealed significant effects of activity ($F_{(2,248)} = 23.8$, $p = 1.52 \times 10^{-8}$) and Pum2 ($F_{(1,248)} = 61.5$, $p = 2.48 \times 10^{-11}$) and a significant interaction between activity and Pum2 ($F_{(2,248)} = 4.0$, $p = 0.02$). The data were further analyzed with a *post hoc* Bonferroni's test. The increase in peak I_{Na} after reduction in Pum2 levels (by shRNA) is greater than that observed after chronic blockade of activity. However, synergy was not observed when both treatments were combined (control, 31.6 ± 1.2 pA/pF; activity block, 44.7 ± 4.1 pA/pF; shRNA–Pum2, 68.3 ± 5.3 pA/pF; combined, 65.2 ± 4.3 pA/pF, $n = 80$, 22, 40, and 45; control vs activity deprived, $p = 0.04$; control vs shRNA, $p = 1.53 \times 10^{-18}$; shRNA vs combined $p = 0.97$; Fig. 5*A*). In contrast, chronic enhancement of activity results in a significant decrease in peak I_{Na}. However, when combined with Pum2 shRNA, we observed no significant change in peak I_{Na} compared with controls (pSUPERIOR transfected, no drug treatment, control, 31.6 ± 1.2; activity enhanced, 15.7 ± 2.2; shRNA–Pum2, 68.3 ± 5.3; combined, 35.4 ± 4.5 pA/pF, $n = 80$, 20, 40, and 17, respectively; control vs activity enhanced, $p = 0.01$; control vs combined, $p = 0.99$; Fig. 5*A*). This supports our hypothesis that Pum2 is required for activity-induced change in I_{Na}. Together, these two observations are also supportive of the model in which activity regulates membrane excitability through alteration of Pum2 level.

To further confirm that these alterations in excitability were the result of changing Pum2 expression levels, we performed immunocytochemistry. Two-way ANOVA showed significant effects of activity ($F_{(2,276)} = 31.9$, $p = 3.52 \times 10^{-3}$) and Pum2 ($F_{(1,276)} = 70.2$, $p = 2.78 \times 10^{-15}$) and a significant interaction between activity and Pum2 ($F_{(2,276)} = 13.9$, $p = 1.78 \times 10^{-6}$). *Post hoc* Bonferroni's testing revealed that Pum2 immunofluorescence intensity was significantly decreased in neurons transfected with shRNA–Pum2 and when combined with activity deprivation (control, 17,053.0 ± 1132.8 pixel intensity units; shRNA–Pum2, 7699.5 ± 406.8 pixel intensity units; combined, 8366.0 ± 691.6 pixel intensity units, $n = 21$, 20, and 21, respectively; control vs shRNA, $p = 3.71 \times 10^{-8}$; control vs combined, $p = 7.01 \times 10^{-7}$; Fig. 5*B*). However, when both treatments were combined, Pum2 immunofluorescence intensity was not significantly different, further showing that the effects of both are not synergistic ($p = 0.99$, shRNA vs combined). In contrast, chronic

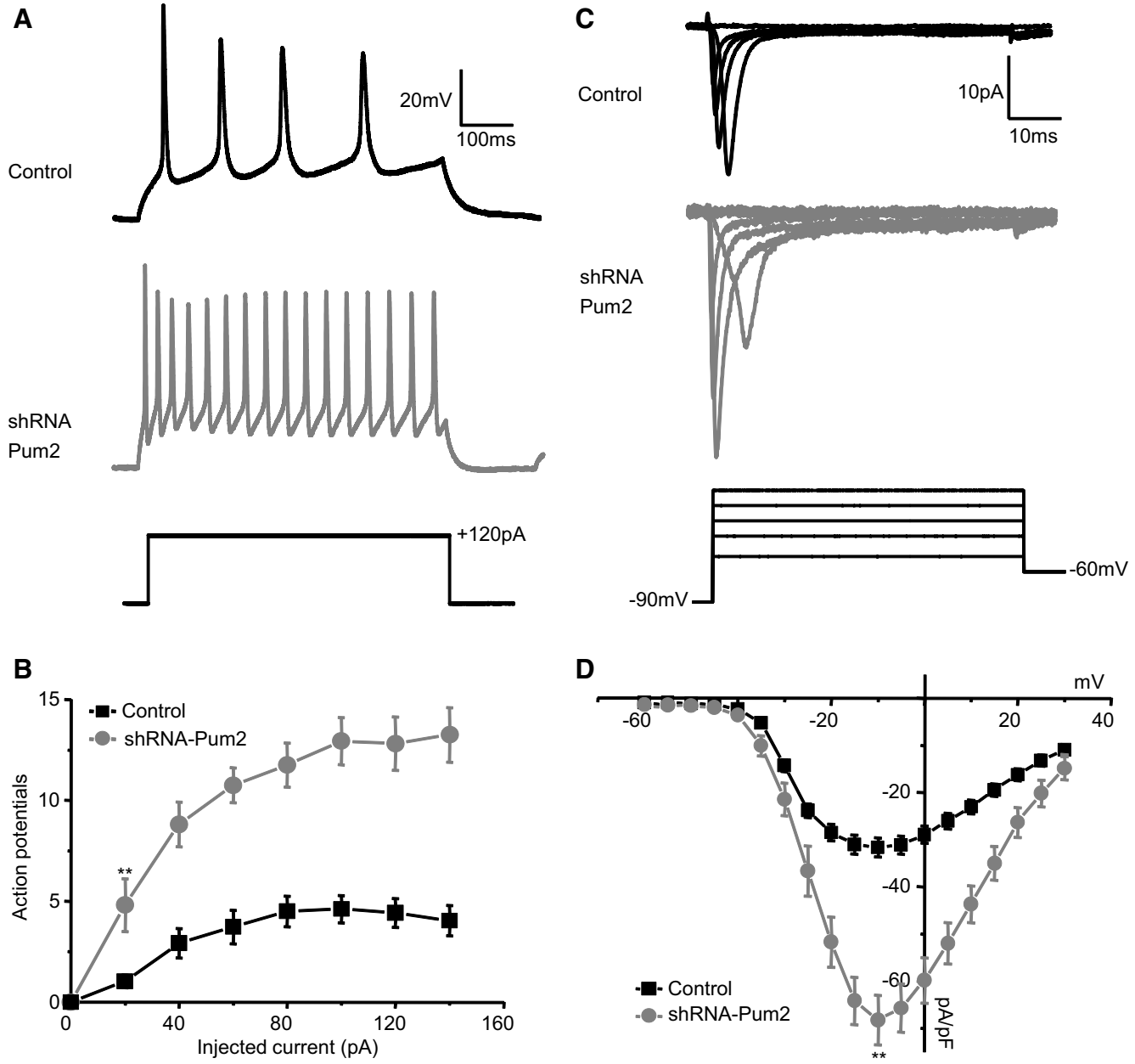

Figure 4. Reducing Pum2 expression increases intrinsic neuronal excitability and I_{Na}. ***A***, Representative action potential firing evoked by a 120 pA/500 ms current injection in pyramidal cortical neuron transfected with either control vector (empty pSUPERIOR; top black trace) or shRNA against Pum2 (bottom gray trace). ***B***, Input– output plot showing the average number of action potentials versus amplitude of current injection shows a highly significant increase in the number of action potentials fired at each injected current compared with control. Data shown are means ± SE, $n \geq 8$. $^{**}p \leq 0.01$, the first-level at which changes in action potential number are significantly different (*t* test). ***C***, Representative voltage-clamp recordings of I_{Na} in control neurons (top black trace) and neurons transfected with shRNA against Pum2 (bottom gray trace). Voltage steps shown are to $V_m = -45, -25, -10, 5$, and 25 mV, respectively. ***D***, Current–voltage plots for I_{Na} measured after neurons were transfected with either control empty vector or shRNA against Pum2. Data shown are means ± SEM, $n \geq 40$. $^{**}p \leq 0.01$, peak I_{Na} is significantly different from control (*t* test).

enhancement of activity (gabazine) results in a significant increase in Pum2 immunofluorescence intensity. When activity enhancement was combined with shRNA–Pum2 transfection, we observed no significant change in Pum2 immunofluorescence intensity compared with control levels (control, 17,053.0 ± 1132.5 pixel intensity units; shRNA–Pum2, 7699.5 ± 406.8 pixel intensity units; combined, 11,999.3 ± 1002.3 pixel intensity units, $n = 21$, 20, and 12, respectively; control vs shRNA, $p = 3.71 \times 10^{-8}$; control vs combined, $p = 0.20$; Fig. 5*B*). Controls are normalized to 1.0 in Figure 5*B*. Finally, plotting peak I_{Na} versus Pum2 immunofluorescence intensity shows a linear and inverse relationship across a range of manipulations, consistent with, and supportive of, Pum2 directly regulating I_{Na} density (Fig. 5*C*). A caveat to interpretation of immunocytochemistry is the qualitative aspect of the analysis of staining intensity. However, when considered together with our quantitative voltage-clamp data, these results suggest that Pum2 is not only sufficient, but also necessary, for activity-dependent regulation of membrane excitability in cortical pyramidal neurons.

Pum2 binds $Na_v1.6$ mRNA

Our results are consistent with a model in which Pum2 acts in an activity-dependent manner to repress the translation of Na_v transcripts in mammalian neurons. In contrast to *Drosophila*, the

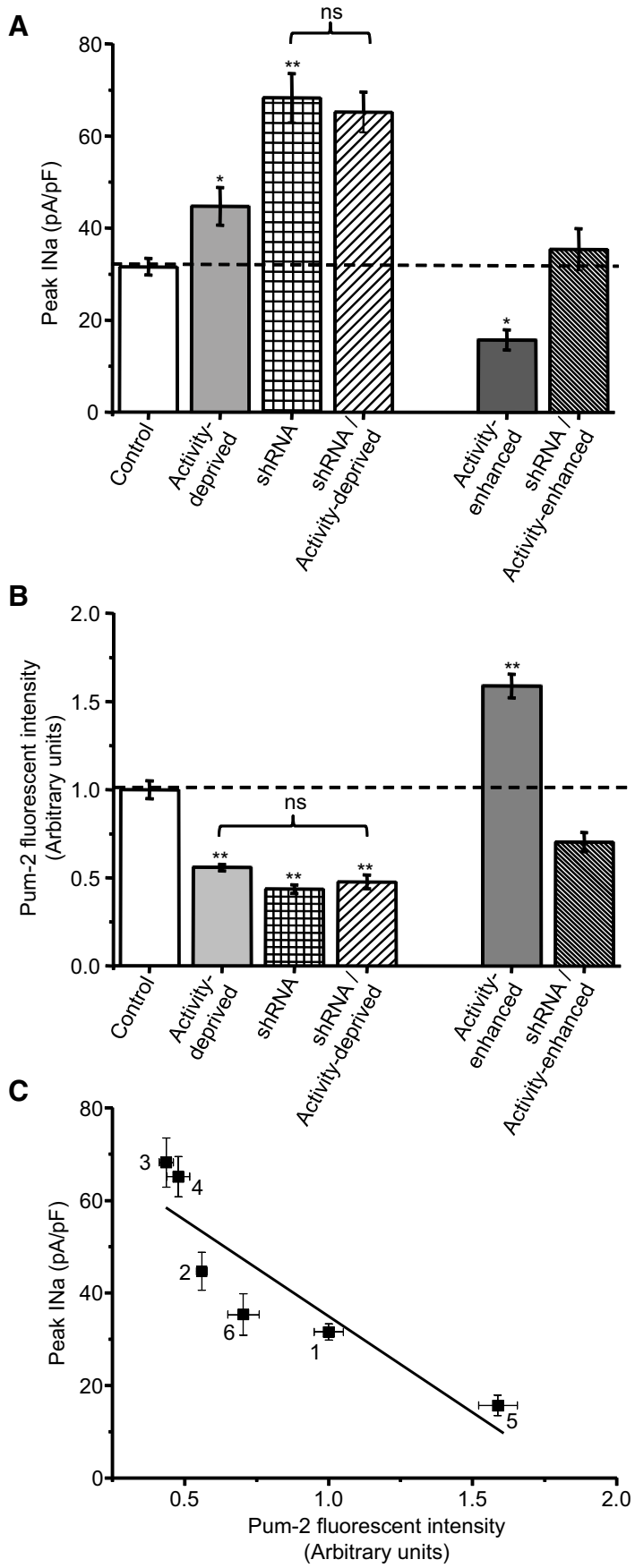

Figure 5. The effect of Pum2 and activity are not synergistic. ***A***, Averaged values of peak I_{Na} recorded in cortical pyramidal neurons after activity deprivation, activity enhancement, Pum2–shRNA, and combined treatments. The effects of activity deprivation and reduced expression of Pum2 (shRNA) on I_{Na} are not synergistic. The reduction in I_{Na} after activity enhancement is prevented by combining this treatment with Pum2 shRNA. Data shown are means ± SEM, $n \geq 17$. $^{*}p \leq 0.05$ and $^{**}p \leq 0.01$ relative to control values (Bonferroni's *post hoc* test after a two-way ANOVA). ***B***, Pum2 immunofluorescence intensity (measured in the cell body) of cortical pyramidal neurons also shows that the reduction in expression seen with activity deprivation or Pum2 shRNA are not synergistic in combination. Simultaneous reduction of Pum2 levels (shRNA) prevents the large increase observed in immunofluorescence attributable to activity enhancement. Data shown are means ± SEM, $n \geq 12$. $^{**}p \leq 0.01$ relative to control values (Bonferroni's *post hoc* test after a two-way ANOVA). ***C***, Peak I_{Na} is inversely proportional to Pum2 immunofluorescence intensity indicative of a correlation between the two (weighted total least squares, $r = 0.93$). 1, Control; 2, activity deprived; 3, shRNA–Pum2; 4, shRNA–Pum2/activity deprived; 5, activity enhanced; and 6, shRNA–Pum2/activity enhanced.

mammalian brain expresses several different Na_vs, and we were interested to test which ones may be targeted by Pum2. To do so, we first established the pattern of Na_V subtype expression in cortical pyramidal neurons used for our recordings.

Using RT-PCR, we observed robust expression of *$Na_V1.1$*, *$Na_V1.2$*, *$Na_V1.3$*, and *$Na_V1.6$* mRNA in visual cortex (Fig. 6*A*). In contrast, we could only detect *$Na_V1.6$* expression in cortical pyramidal neurons (Fig. 6*B*). To establish whether Pum2 could potentially bind *$Na_V1.6$* mRNA, we performed a bioinformatic search using two sequences; the Pumilio regulatory element (PRE; UGUAAAUA) and the NRE (GUUGU) (Murata and Wharton, 1995; Gerber et al., 2006). This search revealed one exact match to the PRE and several matches for the NRE in the open reading frame (ORF) of *$Na_V1.6$* (H.E.D. and R.A.B., unpublished results). To experimentally show whether Pum2 directly binds *$Na_v1.6$* mRNA, we immunoprecipitated Pum2 using an affinity-purified Pum2 antibody, from whole-brain lysate and subjected the eluted RNA to RT-PCR to test for the presence of *$Na_V1.1$*, *$Na_V1.2$*, *$Na_V1.3$*, *$Na_V1.5$*, *$Na_V1.6$*, and *$Na_V1.8$*. Our pull-down clearly showed that Pum2 associates with only *$Na_v1.6$* (Fig. 6*C*). We did not observe any other Na_vs in our pull-downs, although it has been reported that Pum2 binds to *$Na_v1.1$* from rat brain lysates (Vessey et al., 2010). Control pull-downs, using a pan-Na_v antibody, did not immunoprecipitate any *Na_v* transcripts.

To confirm that *$Na_v1.6$* is a target of activity-dependent regulation in cortical pyramidal neurons, we determined whether $Na_V1.6$ expression is altered after chronic block of either synaptic excitation (NBQX/AP-5) or inhibition (gabazine). To do so, we

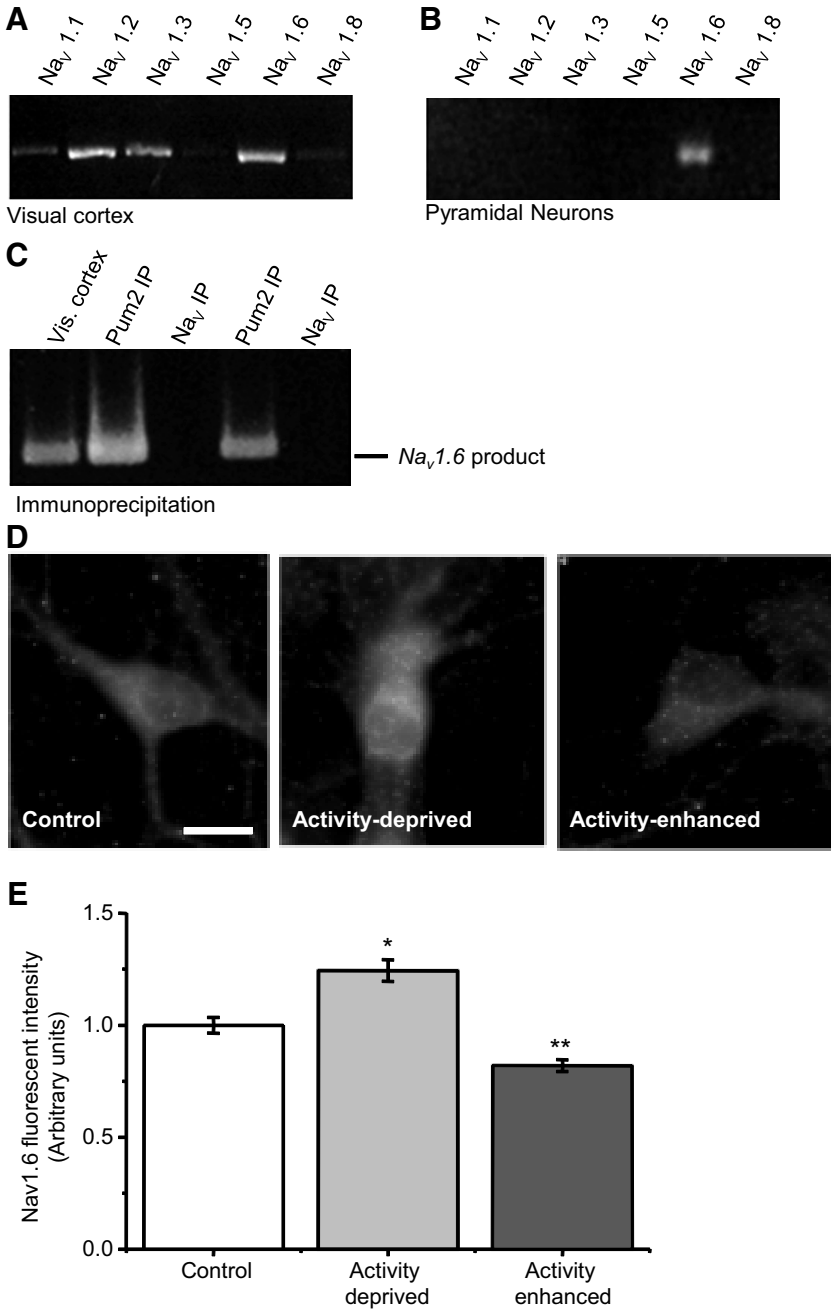

Figure 6. Pum2 binds *$Na_V1.6$* mRNA and decreases $Na_V1.6$ expression. ***A***, PCR from visual cortex shows the presence of *$Na_V1.1$* (faint band), *$Na_V1.2$*, *$Na_V1.3$*, and *$Na_V1.6$* mRNA. ***B***, PCR from pooled pyramidal neurons shows only *$Na_V1.6$* mRNA. ***C***, Immunoprecipitation using Pum2 antibodies (Pum2 IP) was sufficient to pull down *$Na_V1.6$* mRNA. In contrast, immunoprecipitation using a pan-Na_v antibody (Na_v IP) did not pull down any Na_v transcripts. A lysate of visual cortex is also shown (Vis. cortex, far left lane) that was not subjected to immunoprecipitation. ***D***, Immunofluorescence of cortical pyramidal neurons stained with $Na_v1.6$ antibody shows an increase in signal intensity in activity-deprived neurons(middle image) and a decrease in activity-enhanced neurons (right image) compared with controls (left image). Scale bar, 50 μm. ***E***, Averaged data show that activity deprivation increases antibody-specific $Na_v1.6$ immunofluorescence by 25% and activity enhancement decreases immunofluorescence by 22%. Immunofluorescence intensity measurements (measured at the cell body) were performed at the same time and are normalized for cell surface area (for details, see Materials and Methods). Data shown are means ± SEM, $n \geq 24$. *$p \leq 0.05$, **$p \leq 0.01$ (one-way ANOVA with Bonferroni's *post hoc* comparison test).

used an $Na_v1.6$-specific antibody coupled to immunofluorescence. The averaged $Na_V1.6$ immunofluorescence signal intensity was significantly increased in activity-deprived neurons compared with control, nontreated neurons (~25%: 21,589.9 ± 789.0 vs 17,217.1 ± 607.8 pixel intensity units, deprived vs control, $n = 24$ and 32, $p = 4.44 \times 10^{-5}$; Fig. 6*D*,*E*). In contrast, in cultures in which neurons were exposed to enhanced synaptic activity (gabazine), $Na_V1.6$ fluorescence intensity was decreased compared with control, nontreated neurons (~22%: 14,163.3 ± 457.1 vs 17,217.1 ± 607.8 pixel intensity units, enhanced vs control, $n = 24$ and 32, $p = 0.007$; Fig. 6*D*,*E*). Controls are normalized to 1.0 in Figure 6*E*. These results are entirely consistent with, and supportive of, a model in which activity-dependent change in Pum2 regulates membrane excitability through translational repression of *$Na_v1.6$*.

Discussion

Homeostasis acts to stabilize network activity in response to Hebbian-based synaptic plasticity (Turrigiano et al., 1994; Turrigiano, 1999). Our previous work exploited the powerful genetics of *Drosophila* to identify the requirement for Pum, a translational repressor, for homeostatic control of membrane excitability in motoneurons. Pum regulates neuronal excitability by directly binding to and repressing translation of *$DmNa_v$* mRNA that encodes the I_{Na} in this insect (Mee et al., 2004; Muraro et al., 2008). Although it has long been appreciated that mammalian neurons also exhibit this type of homeostatic regulation (Desai et al., 1999), the underlying regulatory mechanism was not known. Here we show that, in cortical pyramidal neurons, I_{Na} changes in an activity-dependent manner, as has been reported previously. Notably, we have investigated the mechanism of this homeostatic regulation and convincingly show that the changes in I_{Na} and hence, in action potential firing, are mediated by Pum2. This strongly suggests that the function of Pum is evolutionarily conserved: *Drosophila* and rat diverged at least 60 million years ago. It also suggests that homeostatic regulation via Pum occupies a predominant role in maintaining stable circuit activity in all nervous systems.

Unlike the relative simplicity of *Drosophila*, which expresses only a single characterized voltage-gated sodium channel gene (*paralytic*), it is perhaps more challenging to fully appreciate how Pum2 may regulate I_{Na} in a mammalian nervous system that expresses multiple sodium channel encoding genes. The mammalian genome encodes a family of 10 voltage-gated sodium α-subunits, $Na_V1.1$–$Na_V1.9$, and an atypical sodium channel termed Na_VX (Yu and Catterall, 2004). Within the CNS, $Na_V1.1$, $Na_V1.2$, $Na_V1.3$, and $Na_V1.6$, encoded by the *scn1A*, *scn2A*, *scn3A*, and *scn8A* genes, are the primary sodium channels (Catterall, 2000; Goldin et al., 2000; Goldin, 2001; Trimmer and Rhodes, 2004). We observed expression of all typical CNS Na_Vs (1.1, 1.2, 1.3, and 1.6) in visual cortex from

which our cultures are derived. However, PCR from the pyramidal neurons from which we record showed that *$Na_V1.6$* expression predominates. It is well known that $Na_V1.6$ is the most abundant Na_V in the output neurons of the cerebellum, cerebral cortex, and hippocampus (Savio-Galimberti et al., 2012). In the CA1 region of hippocampus, $Na_V1.6$ is also the dominant Na_V in the axon initial segments (AIS) and nodes of Ranvier of the pyramidal neurons, with $Na_V1.2$ observed in the proximal part of the AISs (Westenbroek et al., 1989; Krzemien et al., 2000; Lorincz and Nusser, 2010). Pum2 is also widely expressed in mammalian brain (Vessey et al., 2010), indicating that the homeostatic mechanism we report is also likely to be operative in many other brain regions.

In *Drosophila*, Pum function is perhaps best understood from the viewpoint of the establishment of the embryonic anterior–posterior axis involving the translational repression of *hunchback* transcript (Murata and Wharton, 1995). In recent years, Pum has also been reported to be required for normal CNS function, including memory formation (Dubnau et al., 2003), neuron dendrite morphology (Menon et al., 2004; Ye et al., 2004), and glutamate receptor expression in muscle (Menon et al., 2009). In addition to our own previous work showing that Pum is able to regulate I_{Na} in *Drosophila* motoneurons (Mee et al., 2004), these and other observations collectively provide an important mechanistic understanding of Pum. Thus, studies in yeast, *Dictyostelium*, *Caenorhabditis elegans*, *Drosophila*, and *Xenopus* show that Pum proteins are sequence-specific RNA-binding proteins capable of recognizing specific nucleotide sequences in the target mRNAs often, but not always, localized to the 3′ untranslated region (UTR) (Kennedy et al., 1997; Lin and Spradling, 1997; Zhang et al., 1997; Souza et al., 1999; Olivas and Parker, 2000; Parisi and Lin, 2000; Nakahata et al., 2001; Tadauchi et al., 2001; Crittenden et al., 2002). The C-terminal RNA-biding domain is composed of eight tandem repeats, known collectively as the Pumilio homology domain (Zamore et al., 1997; Sonoda and Wharton, 1999; Wang et al., 2002). This domain binds to a conserved consensus 8 nt binding motif [UGUA(A/U/C)AUA (Gerber et al., 2006)] known as the NRE (White et al., 2001) or Pumilio-binding element (Richter, 2010). This highly characteristic sequence has been found in the 3′ UTRs of many, but not all, mRNA targets of Pum (Wickens et al., 2002; Gerber et al., 2004; Bernstein et al., 2005; Opperman et al., 2005). We identified a characteristic 8 nt motif (UGUAAAUA) within the ORF of *$Na_V1.6$*. This mirrors the location of an identical NRE in the *$DmNa_v$* transcript (Muraro et al., 2008). The presence of an NRE in $Na_v1.6$ supports our hypothesis that Pum2 is able to bind the transcript of this gene (the predominant Na_V in mammalian visual cortical neurons). Our analysis of other Na_vs (our unpublished data) show NREs to be additionally present in $Na_v1.1$, $Na_v1.2$, and $Na_v1.7$ indicative of wide-scale regulation by Pum2. Pum2 immunoprecipitation has been reported to pull down *$Na_v1.1$* from rat brain (Vessey et al., 2010).

If Pum2 and its targets are widely expressed, then how is cell-type-specific regulation achieved? The answer to this question may be reliant on cofactors. For example, Muraro et al. (2008) show that, in *Drosophila* CNS, the effect of Pum in regulating I_{Na} requires the cofactor brain tumor (Brat) in some, but not all, neuron types . Equally, translational repression of *cyclin B* requires the established cofactor Nanos but not Brat, whereas translational repression of *hunchback* absolutely requires both cofactors (Sonoda and Wharton, 1999). In mammalian neurons, the requirement for these cofactors in Pum2-dependent translational repression of Na_vs is unknown. Moreover, there are several human homologs of Nanos, termed Nanos 1–3, that are located on chromosomes 10q26.11, 19q13.32, and 19p13.13, respectively (Haraguchi et al., 2003). The potential cofactor Brat is also present in variant copies, termed tripartite motif protein 2 (TRIM2), TRIM3, and TRIM32 located on chromosomes 4q31.3, 11p15.5, and 9q33.1, respectively (El-Husseini et al., 2001; Reymond et al., 2001; Frosk et al., 2002; Sardiello et al., 2008). Few studies have investigated the role of either Nanos or TRIM proteins in mammalian CNS. Perhaps surprisingly, although Nanos1 mRNA has been observed in pyramidal cells of the hippocampus (Haraguchi et al., 2003) and human Nanos1 protein interacts with human Pum2 in a stable complex in germ-line stem cells (Jaruzelska et al., 2003), *Nanos1* knock-out mice show no significant neural defects in terms of their behavior (Haraguchi et al., 2003). This observation was puzzling, because studies in *Drosophila* show a clear requirement for Nanos in Pum-dependent transitional repression of a range of CNS genes, including *$DmNa_v$* and *eIF-4e* (Menon et al., 2004; Muraro et al., 2008). However, genetic redundancy may mask any effects of deleting a single *Nanos* gene in mammals. The simpler genome of *Drosophila* often negates redundancy and in this instance presents the opportunity to further investigate Pum-dependent homeostasis, reassured by the knowledge that a similar, if not identical, mechanism operates in mammalian brain.

An important question that remains unanswered is how synaptic depolarization at the membrane is transduced to activate homeostatic mechanisms. High-frequency burst activity is sufficient to evoke long-term potentiation of intrinsic excitability in layer V pyramidal neurons. This effect is dependent on an influx of extracellular Ca^{2+} and, moreover, can be mimicked by activation of protein kinase A (Cudmore and Turrigiano, 2004). Similarly, a reduction in action potential firing in cultured hippocampal pyramidal neurons, attributable to KCl-induced depolarization, is prevented by the presence of an L-type Ca^{2+} channel blocker but not by antagonism of NMDA receptors (O'Leary et al., 2010). These, and other studies highlight intracellular Ca^{2+} levels as a possible sensor of membrane depolarization (Günay and Prinz, 2010). Changes in gene expression in neurons resulting from activity-mediated Ca^{2+} entry have been extensively described, but no obvious candidates have yet emerged that might link activity to a specific homoestatic response (Miyamoto, 2006). It is also questionable whether a change of I_{Na} density alone is sufficient to alter membrane excitability in the manner reported in this and many other studies: increasing depolarization causing a reduction in I_{Na} and vice versa. Indeed, in a recent modeling study, it was shown that increasing I_{Na} alone unexpectedly reduces firing rate in response to high input current. Only at low current input did the model neurons respond by firing more action potentials (Kispersky et al., 2012). Thus, as shown by Desai et al. (1999), homeostasis likely involves a coordinated alteration of multiple ionic conductances to effect the desired change to membrane excitability. Of course, additional mechanisms probably contribute to activity-dependent homeostasis. For example, chronic depolarization of cultured hippocampal neurons is sufficient to reduce action potential threshold by causing a distal translocation of the AIS away from the soma, an effect that is reversible on returning to normal activity conditions (Grubb and Burrone, 2010a,b).

In summary, we show that activity-dependent regulation of intrinsic excitability in mammalian cortical pyramidal neurons requires Pum2-dependent translational regulation of *$Na_V1.6$* mRNA and that Pum2 is an essential component of the homeo-

static mechanism that allows these neurons to regulate intrinsic excitability.

References

Baines RA (2003) Postsynaptic protein kinase A reduces neuronal excitability in response to increased synaptic excitation in the *Drosophila* CNS. J Neurosci 23:8664–8672. Medline

Baines RA, Uhler JP, Thompson A, Sweeney ST, Bate M (2001) Altered electrical properties in *Drosophila* neurons developing without synaptic transmission. J Neurosci 21:1523–1531. Medline

Bernstein D, Hook B, Hajarnavis A, Opperman L, Wickens M (2005) Binding specificity and mRNA targets of a *C. elegans* PUF protein, FBF-1. RNA 11:447–458. CrossRef Medline

Catterall WA (2000) From ionic currents to molecular mechanisms: the structure and function of voltage-gated sodium channels. Neuron 26:13–25. CrossRef Medline

Catterall WA, Goldin AL, Waxman SG (2005) International Union of Pharmacology. XLVII. Nomenclature and structure-function relationships of voltage-gated sodium channels. Pharmacol Rev 57:397–409. CrossRef Medline

Crittenden SL, Bernstein DS, Bachorik JL, Thompson BE, Gallegos M, Petcherski AG, Moulder G, Barstead R, Wickens M, Kimble J (2002) A conserved RNA-binding protein controls germline stem cells in *Caenorhabditis elegans*. Nature 417:660–663. CrossRef Medline

Cudmore RH, Turrigiano GG (2004) Long-term potentiation of intrinsic excitability in LV visual cortical neurons. J Neurophysiol 92:341–348. CrossRef Medline

Desai NS, Rutherford LC, Turrigiano GG (1999) Plasticity in the intrinsic excitability of cortical pyramidal neurons. Nat Neurosci 2:515–520. CrossRef Medline

Dubnau J, Chiang AS, Grady L, Barditch J, Gossweiler S, McNeil J, Smith P, Buldoc F, Scott R, Certa U, Broger C, Tully T (2003) The staufen/pumilio pathway is involved in *Drosophila* long-term memory. Curr Biol 13:286–296. CrossRef Medline

Ehlers MD (2003) Activity level controls postsynaptic composition and signaling via the ubiquitin-proteasome system. Nat Neurosci 6:231–242. CrossRef Medline

El-Husseini AE, Fretier P, Vincent SR (2001) Cloning and characterization of a gene (RNF22) encoding a novel brain expressed ring finger protein (BERP) that maps to human chromosome 11p15.5. Genomics 71:363–367. CrossRef Medline

Erickson JN, Spana EP (2006) Mapping *Drosophila* genomic aberration breakpoints with comparative genome hybridization on microarrays. Methods Enzymol 410:377–386. CrossRef Medline

Frosk P, Weiler T, Nylen E, Sudha T, Greenberg CR, Morgan K, Fujiwara TM, Wrogemann K (2002) Limb-girdle muscular dystrophy type 2H associated with mutation in TRIM32, a putative E3-ubiquitin-ligase gene. Am J Hum Genet 70:663–672. CrossRef Medline

Gerber AP, Herschlag D, Brown PO (2004) Extensive association of functionally and cytotopically related mRNAs with Puf family RNA-binding proteins in yeast. PLoS Biol 2:E79. CrossRef Medline

Gerber AP, Luschnig S, Krasnow MA, Brown PO, Herschlag D (2006) Genome-wide identification of mRNAs associated with the translational regulator PUMILIO in *Drosophila melanogaster*. Proc Natl Acad Sci U S A 103:4487–4492. CrossRef Medline

Goldin AL (2001) Resurgence of sodium channel research. Annu Rev Physiol 63:871–894. CrossRef Medline

Goldin AL, Barchi RL, Caldwell JH, Hofmann F, Howe JR, Hunter JC, Kallen RG, Mandel G, Meisler MH, Netter YB, Noda M, Tamkun MM, Waxman SG, Wood JN, Catterall WA (2000) Nomenclature of voltage-gated sodium channels. Neuron 28:365–368. CrossRef Medline

Grubb MS, Burrone J (2010a) Building and maintaining the axon initial segment. Curr Opin Neurobiol 20:481–488. CrossRef Medline

Grubb MS, Burrone J (2010b) Activity-dependent relocation of the axon initial segment fine-tunes neuronal excitability. Nature 465:1070–1074. CrossRef Medline

Günay C, Prinz AA (2010) Model calcium sensors for network homeostasis: sensor and readout parameter analysis from a database of model neuronal networks. J Neurosci 30:1686–1698. CrossRef Medline

Haraguchi S, Tsuda M, Kitajima S, Sasaoka Y, Nomura-Kitabayashid A, Kurokawa K, Saga Y (2003) nanos1: a mouse nanos gene expressed in the central nervous system is dispensable for normal development. Mech Dev 120:721–731. CrossRef Medline

Jaruzelska J, Kotecki M, Kusz K, Spik A, Firpo M, Reijo Pera RA (2003) Conservation of a Pumilio-Nanos complex from *Drosophila* germ plasm to human germ cells. Dev Genes Evol 213:120–126. Medline

Kennedy BK, Gotta M, Sinclair DA, Mills K, McNabb DS, Murthy M, Pak SM, Laroche T, Gasser SM, Guarente L (1997) Redistribution of silencing proteins from telomeres to the nucleolus is associated with extension of life span in *S. cerevisiae*. Cell 89:381–391. CrossRef Medline

Kispersky TJ, Caplan JS, Marder E (2012) Increase in sodium conductance decreases firing rate and gain in model neurons. J Neurosci 32:10995–11004. CrossRef Medline

Kole MH, Ilschner SU, Kampa BM, Williams SR, Ruben PC, Stuart GJ (2008) Action potential generation requires a high sodium channel density in the axon initial segment. Nat Neurosci 11:178–186. CrossRef Medline

Krzemien DM, Schaller KL, Levinson SR, Caldwell JH (2000) Immunolocalization of sodium channel isoform NaCh6 in the nervous system. J Comp Neurol 420:70–83. CrossRef Medline

Lin H, Spradling AC (1997) A novel group of pumilio mutations affects the asymmetric division of germline stem cells in the *Drosophila* ovary. Development 124:2463–2476. Medline

Lorincz A, Nusser Z (2010) Molecular identity of dendritic voltage-gated sodium channels. Science 328:906–909. CrossRef Medline

Marder E, Goaillard JM (2006) Variability, compensation and homeostasis in neuron and network function. Nat Rev Neurosci 7:563–574. CrossRef Medline

Mee CJ, Pym EC, Moffat KG, Baines RA (2004) Regulation of neuronal excitability through pumilio-dependent control of a sodium channel gene. J Neurosci 24:8695–8703. CrossRef Medline

Menon KP, Sanyal S, Habara Y, Sanchez R, Wharton RP, Ramaswami M, Zinn K (2004) The translational repressor Pumilio regulates presynaptic morphology and controls postsynaptic accumulation of translation factor eIF-4E. Neuron 44:663–676. CrossRef Medline

Menon KP, Andrews S, Murthy M, Gavis ER, Zinn K (2009) The translational repressors Nanos and Pumilio have divergent effects on presynaptic terminal growth and postsynaptic glutamate receptor subunit composition. J Neurosci 29:5558–5572. CrossRef Medline

Miyamoto E (2006) Molecular mechanism of neuronal plasticity: induction and maintenance of long-term potentiation in the hippocampus. J Pharmacol Sci 100:433–442. CrossRef Medline

Muraro NI, Weston AJ, Gerber AP, Luschnig S, Moffat KG, Baines RA (2008) Pumilio binds para mRNA and requires Nanos and Brat to regulate sodium current in *Drosophila* motoneurons. J Neurosci 28:2099–2109. CrossRef Medline

Murata Y, Wharton RP (1995) Binding of pumilio to maternal hunchback mRNA is required for posterior patterning in *Drosophila* embryos. Cell 80:747–756. CrossRef Medline

Nakahata S, Katsu Y, Mita K, Inoue K, Nagahama Y, Yamashita M (2001) Biochemical identification of *Xenopus* Pumilio as a sequence-specific cyclin B1 mRNA-binding protein that physically interacts with a Nanos homolog, Xcat-2, and a cytoplasmic polyadenylation element-binding protein. J Biol Chem 276:20945–20953. CrossRef Medline

O'Leary T, van Rossum MC, Wyllie DJ (2010) Homeostasis of intrinsic excitability in hippocampal neurones: dynamics and mechanism of the response to chronic depolarization. J Physiol 588:157–170. CrossRef Medline

Olivas W, Parker R (2000) The Puf3 protein is a transcript-specific regulator of mRNA degradation in yeast. EMBO J 19:6602–6611. CrossRef Medline

Opperman L, Hook B, DeFino M, Bernstein DS, Wickens M (2005) A single spacer nucleotide determines the specificities of two mRNA regulatory proteins. Nat Struct Mol Biol 12:945–951. CrossRef Medline

Parisi M, Lin H (2000) Translational repression: a duet of Nanos and Pumilio. Curr Biol 10:R81–R83. CrossRef Medline

Reymond A, Meroni G, Fantozzi A, Merla G, Cairo S, Luzi L, Riganelli D, Zanaria E, Messali S, Cainarca S, Guffanti A, Minucci S, Pelicci PG, Ballabio A (2001) The tripartite motif family identifies cell compartments. EMBO J 20:2140–2151. CrossRef Medline

Richter JD (2010) Translational control of synaptic plasticity. Biochem Soc Trans 38:1527–1530. CrossRef Medline

Sardiello M, Cairo S, Fontanella B, Ballabio A, Meroni G (2008) Genomic analysis of the TRIM family reveals two groups of genes with distinct evolutionary properties. BMC Evol Biol 8:225. CrossRef Medline

Savio-Galimberti E, Gollob MH, Darbar D (2012) Voltage-gated sodium channels: biophysics, pharmacology, and related channelopathies. Front Pharmacol 3:124. CrossRef Medline

Sonoda J, Wharton RP (1999) Recruitment of Nanos to hunchback mRNA by Pumilio. Genes Dev 13:2704–2712. CrossRef Medline

Souza GM, da Silva AM, Kuspa A (1999) Starvation promotes Dictyostelium development by relieving PufA inhibition of PKA translation through the YakA kinase pathway. Development 126:3263–3274. Medline

Spassov DS, Jurecic R (2002) Cloning and comparative sequence analysis of PUM1 and PUM2 genes, human members of the Pumilio family of RNA-binding proteins. Gene 299:195–204. CrossRef Medline

Tadauchi T, Matsumoto K, Herskowitz I, Irie K (2001) Post-transcriptional regulation through the HO 3′-UTR by Mpt5, a yeast homolog of Pumilio and FBF. EMBO J 20:552–561. CrossRef Medline

Tautz D (1988) Regulation of the *Drosophila* segmentation gene hunchback by two maternal morphogenetic centres. Nature 332:281–284. CrossRef Medline

Trimmer JS, Rhodes KJ (2004) Localization of voltage-gated ion channels in mammalian brain. Annu Rev Physiol 66:477–519. CrossRef Medline

Turrigiano GG (1999) Homeostatic plasticity in neuronal networks: the more things change, the more they stay the same. Trends Neurosci 22:221–227. CrossRef Medline

Turrigiano GG, Nelson SB (1998) Thinking globally, acting locally: AMPA receptor turnover and synaptic strength. Neuron 21:933–935. CrossRef Medline

Turrigiano GG, Nelson SB (2004) Homeostatic plasticity in the developing nervous system. Nat Rev Neurosci 5:97–107. CrossRef Medline

Turrigiano G, Abbott LF, Marder E (1994) Activity-dependent changes in the intrinsic properties of cultured neurons. Science 264:974–977. CrossRef Medline

Vessey JP, Vaccani A, Xie Y, Dahm R, Karra D, Kiebler MA, Macchi P (2006) Dendritic localization of the translational repressor Pumilio 2 and its contribution to dendritic stress granules. J Neurosci 26:6496–6508. CrossRef Medline

Vessey JP, Schoderboeck L, Gingl E, Luzi E, Riefler J, Di Leva F, Karra D, Thomas S, Kiebler MA, Macchi P (2010) Mammalian Pumilio 2 regulates dendrite morphogenesis and synaptic function. Proc Natl Acad Sci U S A 107:3222–3227. CrossRef Medline

Wang X, McLachlan J, Zamore PD, Hall TM (2002) Modular recognition of RNA by a human pumilio-homology domain. Cell 110:501–512. CrossRef Medline

Westenbroek RE, Merrick DK, Catterall WA (1989) Differential subcellular localization of the RI and RII Na^+ channel subtypes in central neurons. Neuron 3:695–704. CrossRef Medline

Wharton RP, Struhl G (1991) RNA regulatory elements mediate control of *Drosophila* body pattern by the posterior morphogen nanos. Cell 67:955–967. CrossRef Medline

Wharton RP, Sonoda J, Lee T, Patterson M, Murata Y (1998) The Pumilio RNA-binding domain is also a translational regulator. Mol Cell 1:863–872. CrossRef Medline

White EK, Moore-Jarrett T, Ruley HE (2001) PUM2, a novel murine puf protein, and its consensus RNA-binding site. RNA 7:1855–1866. CrossRef Medline

Wickens M, Bernstein DS, Kimble J, Parker R (2002) A PUF family portrait: 3′UTR regulation as a way of life. Trends Genet 18:150–157. CrossRef Medline

Ye B, Petritsch C, Clark IE, Gavis ER, Jan LY, Jan YN (2004) Nanos and Pumilio are essential for dendrite morphogenesis in *Drosophila* peripheral neurons. Curr Biol 14:314–321. CrossRef Medline

Yu FH, Catterall WA (2004) The VGL-chanome: a protein superfamily specialized for electrical signaling and ionic homeostasis. Sci STKE 2004:re15. CrossRef Medline

Zamore PD, Williamson JR, Lehmann R (1997) The Pumilio protein binds RNA through a conserved domain that defines a new class of RNA-binding proteins. RNA 3:1421–1433. Medline

Zhang B, Gallegos M, Puoti A, Durkin E, Fields S, Kimble J, Wickens MP (1997) A conserved RNA-binding protein that regulates sexual fates in the *C. elegans* hermaphrodite germ line. Nature 390:477–484. CrossRef Medline

Zhang W, Linden DJ (2003) The other side of the engram: experience-driven changes in neuronal intrinsic excitability. Nat Rev Neurosci 4:885–900. CrossRef Medline